Review

Journal of PeptideScience

Received: 1 August 2010 Revised: 12 October 2010 Accepted: 14 October 2010 Published online in Wiley Online Library: 28 December 2010

(wileyonlinelibrary.com) DOI 10.1002/psc.1326

Bioinspired peptide nanotubes: deposition technology, basic physics and nanotechnology applications‡

G. Rosenman,[a]* P. Beker,[a] I. Koren,[a] M. Yevnin,[a] B. Bank-Srour,[a] E. Mishina[b] and S. Semin[b]

Synthetic peptide monomers can self-assemble into PNM such as nanotubes, nanospheres, hydrogels, etc. which represent a novel class of nanomaterials. Molecular recognition processes lead to the formation of supramolecular PNM ensembles containing crystalline building blocks. Such low-dimensional highly ordered regions create a new physical situation and provide unique physical properties based on electron-hole QC phenomena. In the case of asymmetrical crystalline structure, basic physical phenomena such as linear electro-optic, piezoelectric, and nonlinear optical effects, described by tensors of the odd rank, should be explored. Some of the PNM crystalline structures permit the existence of spontaneous electrical polarization and observation of ferroelectricity. The PNM crystalline arrangement creates highly porous nanotubes when various residues are packed into structural network with specific wettability and electrochemical properties.

We report in this review on a wide research of PNM intrinsic physical properties, their electronic and optical properties related to QC effect, unique SHG, piezoelectricity and ferroelectric spontaneous polarization observed in PNT due to their asymmetric structure. We also describe PNM wettability phenomenon based on their nanoporous structure and its influence on electrochemical properties in PNM.

The new bottom-up large scale technology of PNT physical vapor deposition and patterning combined with found physical effects at nanoscale, developed by us, opens the avenue for emerging nanotechnology applications of PNM in novel fields of nanophotonics, nanopiezotronics and energy storage devices. Copyright © 2010 European Peptide Society and John Wiley & Sons, Ltd.

Keywords: peptide nanotubes; vapor deposition technology; quantum confinement; optical absorption and photoluminescence; asymmetric structure; piezoresponse force microscopy and piezoelectric effect; second harmonic generation; wettability; supercapacitors

Introduction

Biological units such as proteins and peptides have the intrinsic ability to self-assemble into elongated solid protein fibers and amyloid fibrils – natural biological nanostructures. Another class of nanomaterials are the man-made bioinspired materials, which are composed of chemically synthesized biomolecules and organized into nanotubes, nanospheres, hydrogels, etc. Having identical biomolecular composition, common molecular recognition and self-assembly mechanisms contain crystalline elementary building blocks organized into similar nanofibrillar structures and can possess common intrinsic physical properties.

Biological Protein Fibers and Amyloid Fibrils-Fine Structure

Nature has developed a vast range of nanostructured materials self-assembled into protein fiber structures [1,2]. They can be divided into two basically different large groups. The first group is related to self-assembled filaments such as actin filaments, myofibrils, microtubules, etc. which provide motility, elasticity, scaffolding and other key properties to living organisms at any scale. These fundamental biological blocks compose collagen and elastic fibrils, and are used to hold the cells together, stabilize and protect them in a human body.

The second group of biological fibers comprises the amyloids, which have been associated to a series of human diseases such

* *Correspondence to: G. Rosenman, School of Electrical Engineering, Iby and Aladar Fleischman Faculty of Engineering, Tel Aviv University, Tel Aviv 69978, Israel. E-mail: gilr@eng.tau.ac.il*

a *School of Electrical Engineering, Iby and Aladar Fleischman Faculty of Engineering, Tel Aviv University, Tel Aviv 69978, Israel*

b *Moscow State Institute of Radioengineering, Electronics and Automation, Prospect Vernadskogo 78, 119454 Moscow, Russia*

‡ *Special issue devoted to contributions presented at the E-MRS Symposium C "Peptide-based materials: from nanostructures to applications", 7-11 June 2010, Strasbourg, France.*

Abbreviations used: *AA, dialanine; AFM, atomic force microscopy; C_{DL}, double-layer capacitance density; DOS, density of states; ESEM, environmental scanning electron microscope; F, phenylalanine; FF, diphenylalanine; FF-PNT, diphenilalanine peptide nanotubes; FW, phenylalanine-tryptophan; HF, hydrofluoric acid; LL, dileucine; L_Z, quantum dimension; MEMS, micro-electro-mechanical systems; NEMS, nano-electro-mechanical systems; PFM, piezoresponse force microscopy; PL, photoluminescence; PLE, photoluminescent excitation; PNM, peptide nanostructured materials; PNT, peptide nanotubes; PNS, peptide nanospheres; SCs, supercapacitors; SEM, scanning electron microscope; SHG, second harmonic generation; RIE, reactive ion etching; QC, quantum confinement; QD, 0D-quantum dot; QW, 2D-quantum well; W, tryptophan; Y, tyrosine; YY, dityrosine.*

Biography

Prof. Gil Rosenman received his M.Sc. Degree in 1970 in experimental physics, his Ph.D. degree in 1975 and Doctor of Science in 1989 (second level of PhD in Russia) both in Solid State Physics from Ural Polytechnic Institute (Yekaterinburg, Russia). In 1990, he immigrated to Israel and joined Faculty of Engineering-Physical Electronics, Tel Aviv University where he is a full professor (2000) and incumbent of the Henry and Dinah Krongold Chair of Microelectronics (2010). He has more than 170 publications and 16 patents. He is well-known for his studies of electron emission from ferroelectrics, physics, and technology of domain engineering for a new generation of lasers, nanoscale polarization inversion, and innovative research in the field of surface modification. Recent activities of his group are centred on a new technology and physics of bioinspired peptide nanostructures, where he developed a new method of deposition, observed quantum confined and ferroelectric phenomena in the nanotubes resulting in development of a new generation of materials for nanophotonics, bio-piezotronics, and recently a new type of energy storage device.

Peter Beker received his B.Sc. degree in Electrical Engineering in 2006 from the Shamoon College of Engineering, Beer Sheva, Israel. He joined Prof. Gil Rosenman's group in 2007 at the Department of Physical Electronics, Tel Aviv University. Currently, he is pursuing his M.Sc. studies and direct entry to Ph.D. program. His research is focused on the studies of bioinspired peptide-based nanostructures materials toward new generation of energy storage devices.

Itai Koren received his B.Sc. in Electrical Engineering from the Technion (Israel Institute of Technology) in 2009, and is now a graduate student pursuing his M.Sc. at the Tel Aviv University under the supervision of Prof. Gil Rosenman in the School of Electrical Engineering – Physical Electronics. His research focuses on bioinspired supramolecular polar peptide nanotubes.

Maya Yevnin received a B.Sc. in Materials Engineering and a BA in Physics from the Technion – Israel Institute of Technology in 2007. She completed her M.Sc. in Materials Engineering in Tel Aviv University in 2009 under the supervision of Prof. Gil Rosenman. She is currently pursuing a Ph.D. in Dr. Yael Roichman's research group at Tel Aviv University.

Biography

Becky Bank Srour, born in 1983 in the United States, moved to Israel in 1987 and completed her B.Sc. in molecular biochemistry and her B.Sc. in chemical engineering at the Technion, Israel Institute of Technology, in 2009. Currently, she is pursuing her M.Sc. in the Material Engineering and Nanotechnology course at Tel Aviv University. Her research is conducted under the supervision of Prof. Gil Rosenman, in the area of biomolecules vapor deposition.

Prof. Elena Mishina is a head of the laboratory of femtosecond optics (Department of Electronics of Moscow Institute of Radiotechniques, Electronics and Atomatization). She has more than 60 publications on nanophotonics and nonlinear-optical characterization of functional materials at International Journals (including Phys. Rev. Lett., Appl. Phys. Lett., Nano Lett., etc.) and six patents of Russian Federation. She is well-known in ferroelectric community for establishing the methods for nonlinear optical characterization of ferroelectric thin films and nanostructures. In 1989, she was awarded Russian State Prize in Physics for Young Scientists. She conducts research with Bi-lateral Russian-Dutch, Russian-German and Russian-Japanese Projects. Recent activities are centered at optical characterization of functional materials and nanostructures (by electro-optical, magneto-optical, and luminescence single-photon and two-photon spectroscopy).

Sergey Semin graduated from Moscow State Institute of Radioengineering, Electronics and Automation (MIREA) in 2007 in electro-optics. He is currently doing his Ph.D. in femtosecond optics group under the supervision of Prof. Elena Mishina. His research is focused on nonlinear optical properties of nanostructures. His main scientific interests are semiconductor nanostructures, organic nanostructures, and photonic crystals.

as Alzheimer's disease, Parkinson's disease, type II diabetes, and some forms of cataract. They are formed when soluble, globular proteins, with diverse sequences and folds, are transformed into insoluble deposits (plaques) [3] that share very similar fine structures [3,4].

Both groups of natural fibrils are characterized by similar self-assembly mechanism leading to supramolecular architectures with highly ordered crystalline structures. The protein fibers [1] can be self-organized at the molecular level into two types of crystal morphology: coiled (coiled-coil) crystals formed by α-helices and crystalline ordered β-sheets [2]. Amyloid fibers are composed of well-ordered β-sheet structures providing strong and stable aggregates. Wide experimental research conducted

Journal of PeptideScience

in the last dozen of years [3–7] has shown that amyloid fibrils share aforementioned-filament nanostructure, irrespective of the origin of their precursor proteins. Their structure consists of stranded-crystalline regions. These elementary blocks are distributed perpendicular to the axis of the fibril and are linked by hydrogen bonds. High-resolution electron diffraction studies have confirmed periodic sub-nanoscale crystalline ordering of the amyloid filaments [5–7]. These fibrillar structures correspond to supramolecular architectures stabilized by noncovalent weak interactions such as hydrogen bonds, van der Waals, hydrophobic, aromatic, electrostatic, and π-stacking [3–7].

Bioinspired Peptide Nanostructures

The development of PNM as a new class of materials was inspired by biological structures [8–11]. Peptide engineering, described by Zhang's concept of 'Peptide Lego' [12], utilizes a combination of the 20 proteinogenic amino acids for the synthesis of a diverse series of nanostructures mimicking the noncovalent interactions found for protein fibers in Nature. The breakthrough in the field came with the observation by Ghadiri *et al*. [13,14] of PNTs formed by the β-sheet-like stacked cyclic peptides. This discovery revealed that fine crystalline regions composed of two peptide subunits form flat ring-shaped conformations. Such ordered arrangements show remarkable axial periodicity and are stabilized by hydrogen bond interactions [15].

Another bioinspired PNM development was aimed to mimic the amyloid fibrils [16–18]. It has been shown that the core recognition motif of the amyloid β protein is the aromatic diphenylalanine element. Reches and Gazit have found that the synthetic dipeptide H–Phe–Phe–OH (FF) and its analogs can self-assemble into well-ordered PNT [16,17] and peptide nanospheres (PNS) [18]. The detailed studies of the crystalline structure of vertically oriented PNT have showed that the original FF-peptide monomers are crystallized into highly ordered nanotube structure possessing sixfold crystalline symmetries. Later, FF-PNT has been related to non-centrosymmetric hexagonal P61 crystal symmetry [19].

The conformational packing problems of 160 simple dipeptides into tubular-like supramolecular structures have been thoroughly analyzed by Görbitz [20–22]. The linkage between the amino acid sequence and the PNT crystal structure became the theoretical guide for peptide-based nanostructure engineering. Görbitz model allows predicting and designing PNT with a definite crystalline symmetry and dimensions, a fine intrinsic structure and shape, and wettability properties, determining their functional properties and consequently nanotechnological applications.

Peptide Nanostructured Materials: Intrinsic Basic Physics

The analyses of a wide research conducted in the last 20 years shows that nanotubular biological and bioinspired materials can be considered as supramolecular structures. The common self-assembly mechanism is responsible for their spatial organization into crystalline building blocks with nanoscale dimensions. The highly ordered arrangements, their crystal symmetry and the conformational packing induce in these structures (i.e. protein fibers, amyloid fibrils and bioinspired peptide nanotubes) exceptional physical properties.

First, the majority of both biomolecules and biomolecular crystals contains neither an inversion of center nor mirror symmetry [23]. Asymmetry of biomolecules and biomaterials was established by Louis Pasteur 150 years ago, and it is considered as their universal intrinsic feature because the structural ordering of the biological systems is the result of a low-symmetry configuration of the elementary cells [24]. Modeling of engineered dipeptides performed by Görbitz [20–22] distinctly showed that bioinspired PNM composed by peptide crystalline subunits comprise also structures without center of symmetry. Such a classification allows observing diverse physical phenomena in PNM, which are described by tensors of odd rank, such as linear electro-optic, piezoelectric, nonlinear optical effects, etc. Another effect which may be predicted is ferroelectricity. Some of the dipeptide structures [20–22] possess crystalline symmetries related to pyroelectric classes. This is a direct evidence of the existence of spontaneous electrical polarization. Peptide molecular dipoles were intensively developed in the last few years by Kimura [25].

Second, the long-term studies on biological filaments and PNM showed that supramolecular ensembles are self-assembled into crystalline regions at nanometer scale. Low-dimensional materials possess exceptional electronic and optical properties related to QC of electrons and holes, being strongly squeezed into a dimension that approaches a critical quantum size, called the exciton Bohr radius. QC is a pronounced quantum mechanical phenomenon which leads to substantial deviation of electron energy spectrum and provides unique optical absorption, exciton luminescence at room temperature and lasing effects [26].

Third, the PNM may create highly porous nanotubes when various hydrophobic residues are packed into a structural network, that form sub-nanoscale hydrophilic channels within the PNT hydrophobic matrix [27]. The specific PNT wettability properties can be exploited for water, ion, and molecule transport.

Thus, we can divide the PNM intrinsic physical properties into the following three groups where each one is associated to a basic physical phenomenon.

(1) QC phenomena (electronic and optical properties such as optical absorption, exciton luminescence, and lasing effect) related to low-dimensional crystalline building blocks forming supramolecular PNM.
(2) Ferroelectric and related phenomena (piezoelectric, SHG, etc.) based on asymmetry of PNM crystalline building blocks.
(3) Wettability phenomenon related to fine conformational structures and nanoporous arrangements of PNM.

In this review, we report on self-assembled bioinspired intrinsic physical PNM properties [28], their new deposition technology, their electronic and optical properties related to QC effect [29–31], as well as on unique ferroelectric and related phenomena [32] such as piezoelectricity [33] and SHG observed in PNT. We also describe PNM wettability properties and electrochemical effects [34]. Our large scale technology of PNT vapor deposition and patterning [28,35], combined with physical effects at nanoscale, opens the avenue to emerging applications of PNM in the new fields of nanophotonics, nanopiezotronics, and energy storage devices.

PNM Deposition and Patterning Technology

PNT Vapor Deposition Method

Valuable methods for the preparation of bioinspired PNM are of a crucial importance to obtain reproducible results in this emerging

field. Until today, the sole method to fabricate PNT was based on the use of aqueous and organic solutions [16–18].

Recently, we developed an alternative method based on a large scale bottom-up technology of PNT coatings by physical vapor deposition [28]. Vapor deposition is one of the basic technologies in microelectronics, and its application to biomolecule deposition [28,36] allows to apply both the fundamental physics of vapor deposition and the established techniques for the development of a robust PNM technology. Atomistic coating technique is based on vaporization process from a solid or a liquid source. The vaporized flux of atoms or molecules is transported through vacuum, low-pressure gaseous environment or plasma toward the substrate where it condenses. In a thermal vapor evaporation process, the source material is heated to a temperature where there is an appreciable vapor pressure. During the deposition of a biomaterial, the monomer powder is placed in the sample holder, directly connected to the heater, allowing the evaporation of the biomaterial at a definite temperature. A substrate is placed on the substrate holder, at a definite distance above the source material. The coating is then formed on the downward side of the substrate.

Several different sorts of peptides were tested and deposited by physical vapor deposition. Vertically oriented peptide tubular coatings were fabricated using both aromatic and nonaromatic peptides, dipeptides and amino acids such as F, FF, W, FW, Y, YY, AA, LL, etc. Figure 1A and E shows the typical top and side views of SEM images of the deposited FF-PNT. SEM shows a normally oriented, homogeneously distributed array of nanotubes with a density of 10^8 cm^{-2}. The FF-PNT has a wide range of diameters, from 50 to $>$300 nm. The nanotube parameters can be varied in a wide range by adjusting the deposition parameters; average height (1–50 μm) and surface density (10^5–$10^8 \cdot cm^{-2}$). In Figure 1A a side view of a thick array of nanotubes (~65 μm) is shown, and in Figure 1B a side view of a thinner array of nanotubes (~20 μm) is shown. This method allows to obtain a dense homogeneous PNT coating using the biological molecules of different origin.

Fine details were found at high-resolution SEM images (Figure 1C and D). Two different sorts of PNT were revealed [34]. The majority of the deposited PNT are closed-top PNT which have a nanobelt shape, whereas a small part of PNT is opened-end hollow PNT. The hollow vertically oriented PNT has been described by Gazit as PNT composed from linear FF dipeptide molecules [17]. Our analysis [34] showed that peptide nanobelts consist of cyclic-FF. As we found, these two sorts of PNT have not only different morphologies but they also possess different crystallographic symmetry, optical properties, wettability, etc.

PNT Patterning

Traditional technology to prepare MEMS and NEMS devices was based on a 'top-down' approach where a wafer or a micrometer scale device is carved, or molded out of a larger bulk material [37]. A 'bottom-up' approach provides an alternative route to the development of nanoscale technology. In the 'bottom-up' process, simple building blocks interact each other in a coordinated way to form ordered structure, as it was shown by deposition methods of PNT [28,29,35] where patterned PNT were used for microfluidic chips and PNT arrays for light emitting devices. However, one of the most significant challenges in the 'bottom-up' approach is the large scale assembly of nanomaterials at well-defined locations on substrates. Much effort has been focused on tackling the controlled assembly of nanotubes by various methods [38].

Here, we describe a novel and simple strategy for a wafer assembly of highly ordered and vertically aligned PNT arrays. The patterned PNT arrays combine the attributes of photolithography with 'bottom-up' self-assembly. Our key solution for selective removing the PNT from desirable surfaces was the use of hydrogen fluoride (HF) to dissolve oxides. In Figure 2 the process for fabrication of the PNT array is outlined. The process begins with standard double-sided polished 100 mm diameter and 500 μm thickness single crystal silicon wafer with thermally grown 5 μm thick silicon dioxide layer (SiO_2) on front and back sides (Figure 2A). By means of the standard photolithography methods and using RIE, the holes of 50 μm in diameter with a 35 μm period were patterned and etched in the SiO_2 upper layer to a depth of 5 μm (Figure 2A–D). At the following stage, the vapor deposition technology of PNT was applied (Figure 2E). As a result, the substrate surface was coated by vertically aligned PNT with the height of about 5 μm (Figure 2A and B). Selective removal of the PNT coating above the SiO_2 layer was accomplished by immersing the specimen in 49% HF at 25 °C for 60 s and rinsing it in water (Figure 2F). The final architecture is composed of the PNT arrays within the substrate holes. Figure 3 shows SEM images of the substrate before (Figure 3A and B) and after (Figure 3C and D) the etching process by HF. It should be mentioned, that the nanotubes completely retained their structure in HF. These results open a new approach for studying the physical properties of PNT in PNT-patterned samples with high density and homogeneous coating.

PNM Optical Properties

PNM are self-assembled into different geometrical shapes at micro- and nanometer scale such as nanotubes, nanobelts, nanospheres, etc. Regardless of their conformational shape, the supramolecular structure is assembled from crystalline peptide subunits [17,39].

Nanoscale materials of different origin are endowed of diverse and new optical properties compared to bulk crystals. They are related to QC phenomena [26] when the material dimensions become comparable to the de-Broglie wavelength of the confined charges. The confinement can be of several orders, whether it is a 2D-QW, 1D-quantum wire or 0D-QD. A scheme of the different confinements compared to the bulk material, along with the electron DOS of each structure is shown in Figure 4.

In QC structures the electron DOS differs dramatically. The crystalline bulk materials are characterized by quasi-continuous variation of DOS as a function of energy (Figure 4). The DOS of 2D structure-QW is described by step-like behavior. Electrons and holes can freely move in *X* and *Y* directions, and their motion is strongly affected by potential discontinuities in the *Z* direction. As a result, the DOS of QW breaks into a series of quantized energy levels. The DOS of QD is characterized by a spike-like behavior (Figure 4). Such a striking alternation of the DOS in QC structures causes dramatic changes of electronic and optical properties that are widely used in the field of light emitting diodes and laser devices.

The powerful tool of QC phenomena studies is optical absorption defined by the electron/hole energy spectrum. The optical absorption coefficient is directly proportional to the DOS and described by a spike-like behavior as a function of photon energy. For a QW structure it is characterized by a step-like function which exactly coincides with its DOS [26].

Optical absorption was studied in three different species of PNM based on FF [29–31]: (i) the Boc-FF peptide self-assembled

Journal of PeptideScience

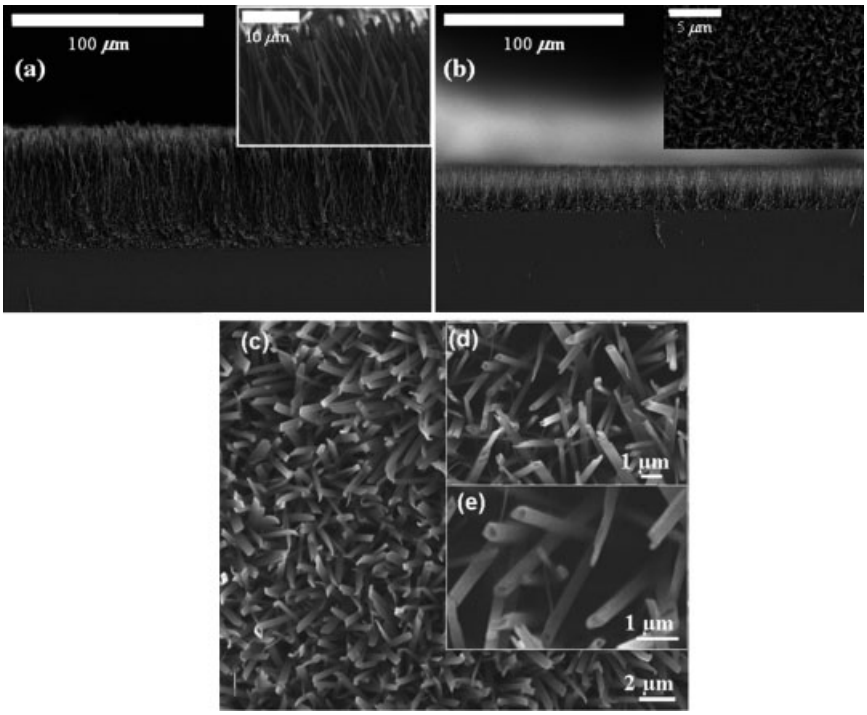

Figure 1. Vapor deposition of PNT. (a) Side view of vertically aligned PNT with the thickness of ~65 μm. The inset shows higher magnification of the image. (b) Side view of vertically aligned PNT with the thickness of ~20 μm. The inset shows a top view SEM image of PNT. (c) High-resolution top-view SEM image of PNT nanoforest after the vapor deposition process. (d, e) The inset shows high-resolution SEM images of an opened-end hollow PNT.

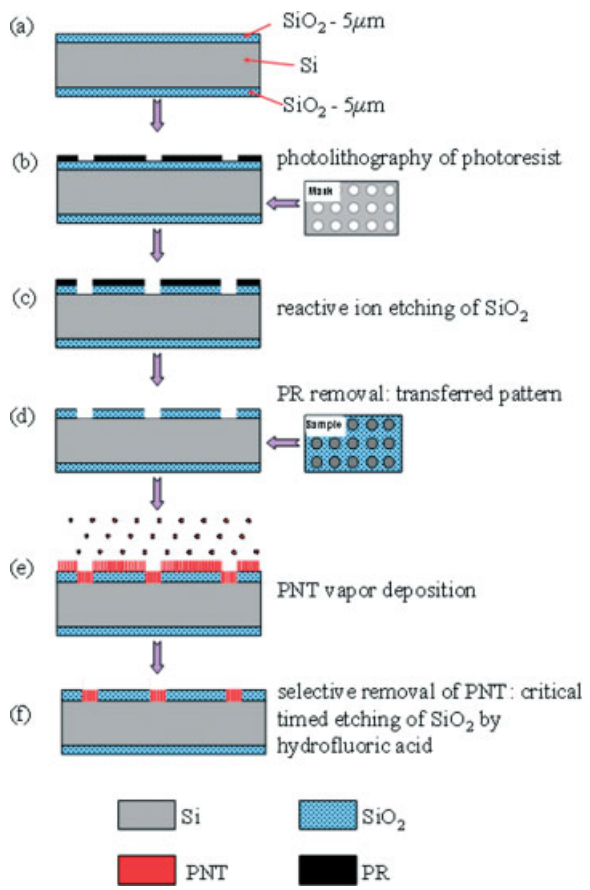

Figure 2. Schematic diagram of the PNT bundles fabrication process.

into nanospheres (PNS) [30], (ii) FF nanotubes deposited by vapor deposition [29], and (iii) Fmoc-FF hydrogel [31].

Figure 5A, C, and E illustrate these three peptide nanostructures. The self-assembly process leads to the formation of PNS structures with a wide diameter range of 40–1 μm (Figure 5A). The vapor deposited FF-PNT (Figure 5C) represents vertically oriented nanotubes with cross-section dimensions, from 100 nm to 0.5 μm and an average height of 20 μm. The hydrogel's network is composed of PNT-hydrogel with a final diameter of 7–15 nm (Figure 5E).

The optical absorption of PNS (Figure 5B) and PNT (Figure 5D) demonstrates completely different graphs of optical absorption coefficient *versus* light wavelength. The PNS optical absorption graphs, recorded for different Boc-FF concentrations (Figure 5A), presents a few separated peaks. The position of the individual peaks and the spectral structure of the optical absorption curves do not change with the peptide monomer concentration, while the intensity of the peaks increases with concentration. All optical absorption data (Figure 5) were combined with PL measurements [29–31]. We found that both absorption and PL excitation (PLE) spectra are identical. The peaks are located at 265 nm (4.68 eV), 259 nm (4.79 eV), 253 nm (4.90 eV), and 248 nm (5.0 eV). The energy interval between two neighboring peaks, both for absorption and for PLE, is the same and equal to 0.10–0.11 eV (Figure 5B).

The optical absorption properties are completely defined by the electron/hole energy spectrum [26]. The electron DOS of a 0D structure-QD is described by a spike-like behavior (Figure 4). Our PNS optical absorption spectra (Figure 5B) have identical spike-like features that confirm the direct evidence for the formation of QD structures in a self-assembled PNS (Figure 5A and B) [30].

In Figure 5D, the absorption spectrum of PNT is reported in comparison with FF monomers in aqueous solution. In contrast

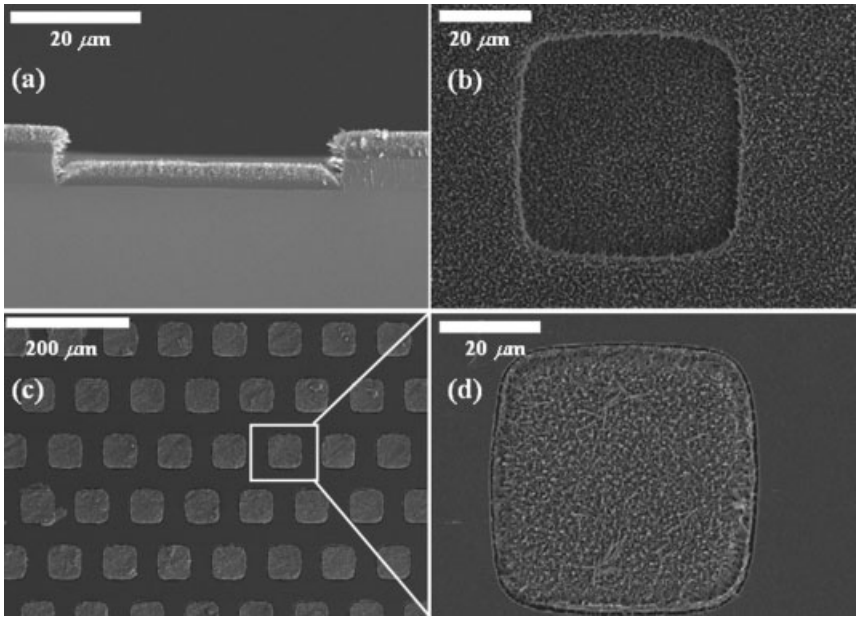

Figure 3. SEM images of patterned arrays of PNT fabricated by vapor deposition technology. (a) Cross-section view of patterned substrate covered by PNT coating. (b) Top view of the patterned substrate covered by PNT coating. (c) Top view of PNT bundles after HF release. (d) Enlargement view of PNT bundle image. (PR-photoresist).

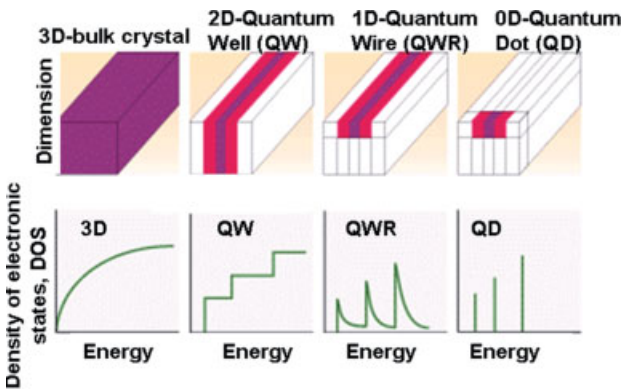

Figure 4. Density of electronic states (DOS) of the bulk substance in comparison to the quantum confined structures: 2D-QW, 1D-quantum wire and 0D-QD.

to the spectrum of the monomer, which exhibits a peak at 257 nm, the absorption spectrum of the vertically aligned FF-PNT is characterized by two distinguished bands located at 245–264 and 300–370 nm (Figure 5D). The recorded step-like optical absorption behavior for FF-PNT (Figure 5D) clearly indicates the existence of 2D-QW crystalline structures, embedded in the FF-PNT during self-assembly vapor deposition.

The hydrogel optical absorption contains both types of quantum confined regions. Small concentrations of Fmoc-FF peptide monomer related to a sub-gel state are described by a spike-like structure (Figure 5F). For high concentrations of the peptide monomer the absorption spectrum is transformed into a pronounced step-like spectrum. Our microscopic data indicated the generation of the hydrogel's network only for high monomer concentrations (Figure 5E). Thus, comparing the data for PNS (Figure 5B) and PNT (Figure 5D) with those observed for the hydrogel (Figure 5F), we may assume that low sub-gel concentration of peptide monomer is self-assembled into QD, while at higher concentrations the QD are finally transformed into QW structures (Figure 5F).

These experimental data on QC phenomena show that, regardless of the micrometer shapes of peptide spheres, nanotubes or hydrogels, they are composed of highly ordered crystalline peptide blocks. The calculation of the dimensions of these quantum confined regions, L_Z, is of fundamental interest, and allows for better understanding of fine peptide nanostructures, shapes, and size of the elementary components. Such low-dimensional QD and QW are characterized by strengthening of the Coulomb interaction 'electron-hole', and the creation of an exciton-electron/hole neutral pair, whose binding energy ΔE_{exc} allows for direct estimation of the L_Z [26].

For the three PNM (Figure 5), the exciton peak may be found at the long wavelength edge of the optical absorption spectra of QW. Such exciton absorption peak was particularly pronounced for QW of the hydrogel (Figure 5F). The exciton binding energy for QD composed of PNS structures [30] was ΔE_{exc} ~0.44 eV; QW structures of vapor deposited PNT [29] are characterized by ΔE_{exc} ~0.98 eV while ΔE_{exc} ~0.31 eV was found for QW of hydrogel PNT [31]. The implemented theoretical calculations of L_Z afforded values in the range of a few nanometers (L_Z = 1.2–2.6 nm) [29–31]. A comparison of this key parameter with the lattice constant of crystalline FF, [27] with one of the axis around 0.5 nm, allows to conclude that 2–3 crystal unit cells compose of the peptide building block in the low-dimensional QC direction.

It should be emphasized that the found energies in the QC bioinspired peptide nanostructure are two orders of magnitude higher than those in semiconductor GaAs. Such tightly bound excitons are responsible for the pronounced room temperature PL observed in these PNM [29–31]. PNS and peptide hydrogels display intensive PL in the UV range limited at the 'red' edge. However, vapor deposited PNT also show a strong blue PL seen through naked eye (Figure 6B). This unique property is the basis

Journal of PeptideScience

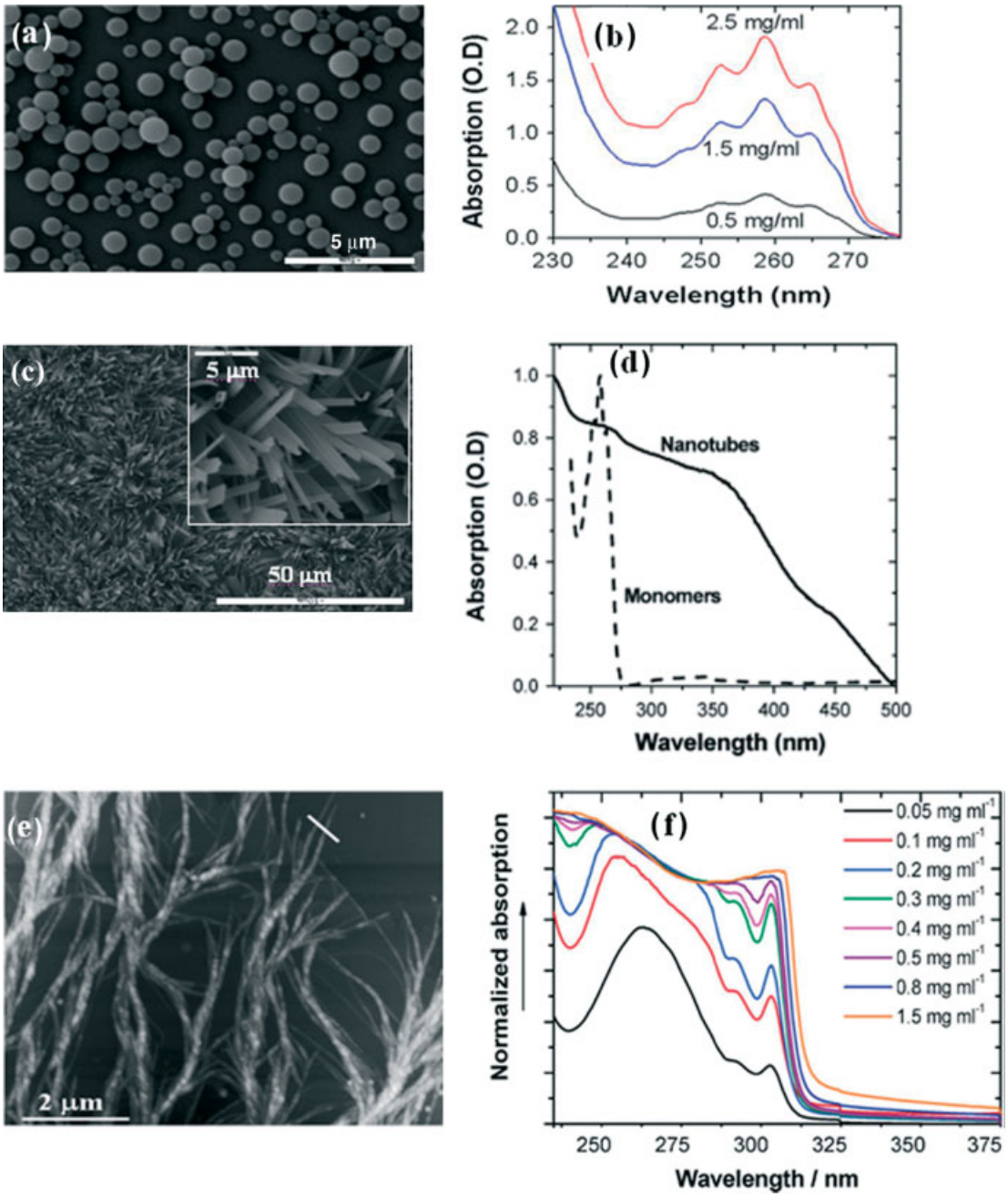

Figure 5. (a) SEM images of the Boc-FF PNS; (b) optical absorption of Boc-FF PNS; (c) SEM image of vapor deposited PNT; (d) optical absorption of vapor deposited FF-PNT; (e) SEM image, morphology of Fmoc-FF hydrogel; (f) optical absorption of Fmoc-FF hydrogel.

for new light sources such as light emitting diodes which were first demonstrated by Amdursky [29] (Figure 6C).

Studies of the optical properties allow direct observation of quantum confined regions in self-assembled PNM. These QC domains define a fine structure of PNM where elementary components are nanocrystalline regions of a specific geometry. Thus, we may assume that QD found in PNS are small crystalline balls. QW observed in vapor deposited PNT and peptide hydrogels are elementary crystalline building blocks forming a fine structure of PNT and representing thin crystalline plates.

It should be emphasized that intrinsic QW structures are the basis for the development of a new generation of QW lasers of biological origin.

Ferroelectric and Related Phenomena in PNM

The symmetry analysis predicts basic physical properties of dielectric crystals [40]. Ferroelectric and related phenomena such as piezoelectric and SHG are observed in crystalline dielectrics related to 20 noncentrosymmetric crystallographic groups. High structural order in biological systems combed with their intrinsic helical or chiral asymmetry provides low-symmetry crystalline configurations at any level [23] from amino acids [41] to bones [24]. Asymmetric crystalline structure in biological materials allowed the observation of piezoelectric effect and SHG in plants, animal and human tissues [41–44]. Reports on pyroelectric effects and existence of macroscopic spontaneous electrical polarization in

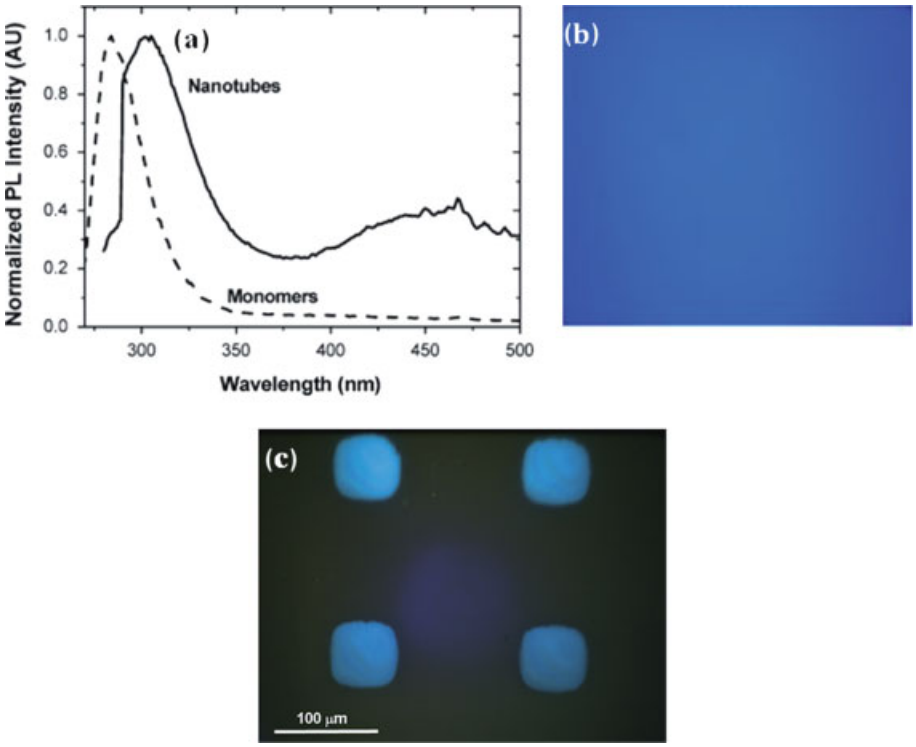

Figure 6. (a) PL of FF-PNT (solid line) and FF monomers (dashed line); the excitation wavelength was 260 nm;(b) blue PL image of homogeneous PNT array deposited by vapor deposition technology; (c) PNT-light emitting devices (patterned array).

bones were the first evidence of the ferroelectricity in biological tissue [24].

Understanding the relationship between physiologically generated electric fields and mechanical properties (piezoelectric effect) has become the main motivation of studying piezoelectricity in protein fibrils. Local piezoelectric behavior and structural imaging using sub-10 nm high-resolution PFM technique applied to a variety of protein-based materials, including tooth, antler, and cartilage has been demonstrated [45–48]. Pronounced electromechanical response was ascribed to a protein (presumably collagen) embedded within a non-piezoelectric matrix. Recently, Gruverman *et al*. [46] reported that fibrils in fascia tissues within parallel bundles can have opposite polar axis orientation. The piezoelectric effect was recently observed by Kalinin [47] in amyloid fibrils, produced from bovine insulin, by using a newly developed technique, which measures electromechanical coupling in liquid environment applying a broadband electrical excitation.

Piezoelectric Properties of PNT

An analysis of a wide range of bioinspired dipeptides showed that they are packed into a crystalline arrangement with no center of symmetry [21]. The piezoelectric effect was studied in two dipeptide nanotubes (FF and LL). According to the Görbitz's classification [27] both peptides can self-assemble into PNT and are crystallized into asymmetric crystal structures: FF adopts a hexagonal crystal system (space group $P6_1$) and LL is related to an orthorhombic crystal system (space group $P2_12_12_1$). Both PNT were prepared by self-assembly from aqueous (horizontally oriented tubes) and organic (normally oriented tubes) solutions. Optical images of the normally oriented PNT confirm their hexagonal (FF) and orthorhombic (LL) crystal symmetry (Figure 7).

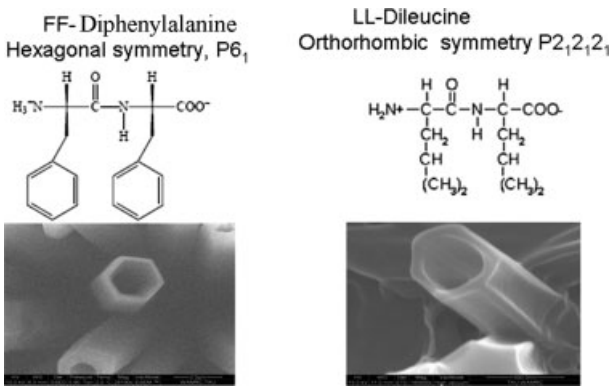

Figure 7. Optical images of aromatic FF (hexagon symmetry) and nonaromatic LL (orthorhombic symmetry) dipeptide nanotubes.

The first observation of the piezoelectric effect in FF-PNT using PFM was recently reported in our work in cooperation with Kholkin's group [33]. The third rank tensor of the FF-PNT $P6_1$ space group is:

$$\begin{pmatrix} \varepsilon_{11} \\ \varepsilon_{22} \\ \varepsilon_{33} \\ 2\varepsilon_{23} \\ 2\varepsilon_{13} \\ 2\varepsilon_{12} \end{pmatrix} = \begin{pmatrix} 0 & 0 & d_{13} \\ 0 & 0 & d_{31} \\ 0 & 0 & d_{33} \\ d_{14} & d_{15} & 0 \\ d_{15} & -d_{14} & 0 \\ 0 & 0 & 0 \end{pmatrix} \begin{pmatrix} E_1 \\ E_2 \\ E_3 \end{pmatrix} \quad (1)$$

The tensor matrix shows that applying an E_3 electric field (along the tube axis) the longitudinal d_{33} piezoelectric coefficient (out-of-plane component) can be measured. Owing to the limitation of the AFM and strong mechanical flexibility, we could not measure

Journal of PeptideScience

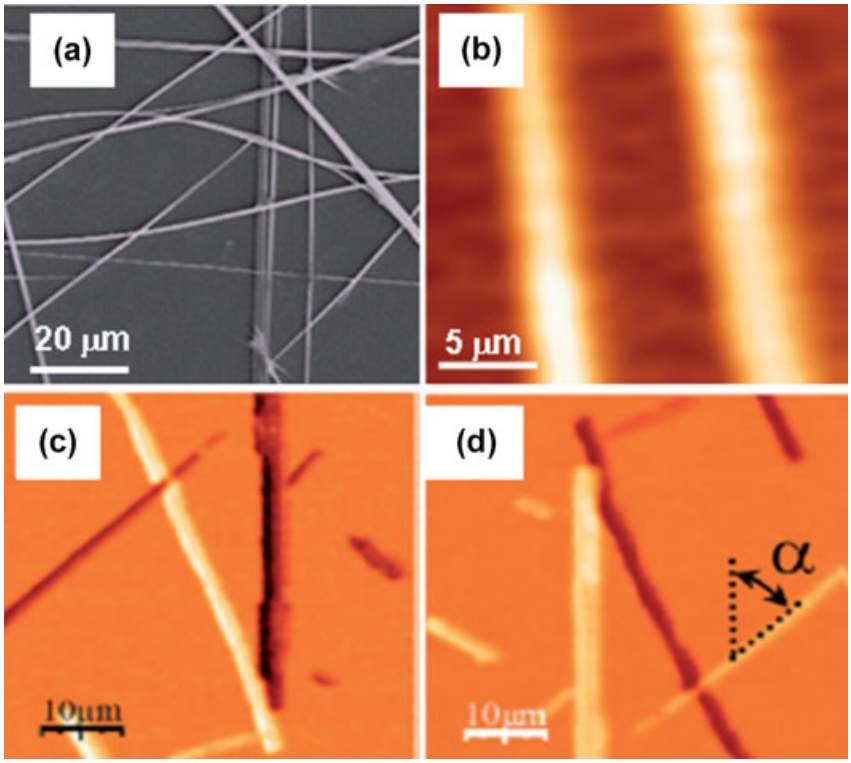

Figure 8. Optical (a) and AFM topography (b) images of FF-PNT; (c) piezoelectric response image of oriented in-plane FF-PNT due to shear piezoelectric effect; (d) the same response after physical rotation by 180° of the sample.

the PFM response of normally standing tubes but we were limited to only horizontally oriented tubes. The piezoelectric tensor has zero d_{11} and d_{22} piezoelectric coefficients. By applying E_1 (or E_2) we did not find a piezoelectric signal. However applying E_1 (which is the same as E_2 due to the tube symmetry) we measured the d_{15} shear component coefficient (in-plane component). Figure 8 shows shear piezoelectric response of the FF nanotubes along with fragments of optical images and AFM topography. Two kinds of nanotubes ('black' and 'white') are the evidence of the opposite sign of the piezoelectric coefficients for the different PNT (Figure 8C). To validate these results, the sample was physically rotated by 180° (Figure 8D) and the PFM contrast changed; the 'black' tubes became 'white' and vice versa. This simple experiment shows that PNT have unique polar direction along the PNT axis. The observation of a spontaneous polarization in FF-PNT is supported by their crystalline symmetry where pyroelectric properties and electrical polarization are permitted.

Piezoelectric phenomenon is a linear dielectric effect [40] and its response signal should be linear with the applied electric field bias. In Figure 9 the 'in-plane' shear piezoelectric response is reported at various biases, from 0 to 14 V. The result shows a linear response between the piezoelectric response and the applied voltage. The direct measurement of the FF-PNT piezoelectric coefficient value is problematic because of the complex distribution of the applied electric field in the hollow nanotube. The PNT piezoelectric coefficient was found by comparison with well-known piezoelectric $LiNbO_3$ and lateral signal calibration, giving a value about 60 pm/V (shear response for tubes of 200 nm in diameter). It should be emphasized that piezoelectric coefficients measured in biological tissues showed values nonexceeding 2 pm/V [46–48].

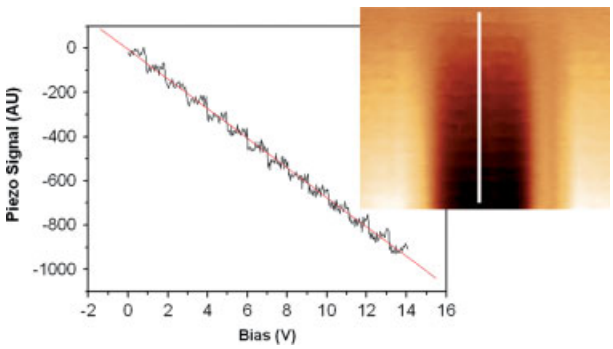

Figure 9. Bias dependant of the in-plane (shear) piezoelectric signal. The graph shows a cross-section along the white line at the PFM image. At the measurement, the bias on the tip was changed by 1 V for every 1 min, from 0 to 14 V.

The piezoelectric effect was also studied by us in LL-PNT (Figure 7) and the PFM experimental results showed the existence of pronounced shear piezoelectric effect. A sharp variation of the piezoelectric contrast indicating a possible existence of the exceptional polar direction was found also in these PNT.

Second Harmonic Generation in FF-PNT

SHG is related to a nonlinear electron phenomenon observed in ordered structures with no center of symmetry. SHG effect was used in biological studies and found in the pineal gland [44]. Intrinsic and highly noncentrosymmetric protein fibers are intensively studied by two-photon spectroscopy to assess the presence of SHG. Nonlinear excitation is an attractive tool for high-resolution imaging of natural fibril structures (i.e.

collagen, microtubules, myosin, etc). Fibrillar collagen, possessing a noncentrosymmetric structure is characterized by a very high nonlinear susceptibility. The SHG of collagen produces extremely bright signals, providing an imaging of the fine structure in the tissues at submicron resolution [49,50].

The SHG method was applied in our laboratory to FF-PNT with a nonlinear optical excitation by using a 100-femtosecond laser with high pulse power density up to 1 GW/cm^2 (pulse energy density up to 100 μJ/cm^2). Two-photon excitation spectroscopy of SHG was studied at the spectral wavelength of 800 nm (Figure 10) and it consists of a narrow second harmonic peak generated at 800 nm, which is the first evidence for the existence of a ferroelectric-related phenomenon in FF-PNT. Detailed studies showed that for low power the SHG intensity is quadratic *versus* the excitation light power. Measured nonlinear optical susceptibility of PNT is very high and reach $\chi_{PNT} = 20$ pm/V, comparable to the best inorganic nonlinear materials like $LiNbO_3$ and $LiTaO_3$.

Wettability Effects in Bioinspired PNT

Wettability (hydrophobic/hydrophilic) properties depend on fine structure of biological fibers and bioinspired dipeptide nanotubes. Being one of the basic parameters in weak interactions, present in supramolecular structures, this property is crucial for understanding the transport of water, ions and large molecules across biological membranes. Theoretical research on design and modeling of dipeptide nanotubes of different origin inspired the synthesis of self-assembled microporous peptide materials possessing chiral hydrophilic nanochannels of about 10 Å in diameter [19–22]. Another aspect associated to PNM wettability is the emerging application of PNT toward the production of micro- and nanofluidic chips and superhydrophobic coatings [28,51]. A superhydrophobic surface was developed by growing the peptide nanowire film in the presence of pentafluoroaniline at high temperatures [51]. It has been found that the superhydrophobic characteristics of the film originated from an increased nanoscale roughness and the decreased surface free energy through the incorporation of pentafluoroaniline molecules into the peptide.

An important practical aspect of PNT wettability is the development of a new generation of energy storage devices-SCs [28,34], where the wettability strongly influences the formation of electrical double layers. The knowledge of the wettability properties is highly limited. We have studied this characteristic on FF-PNT aiming to the design of SCs with PNT-modified electrodes of superior properties [28,34].

The research was conducted using FF-PNT arrays prepared by physical vapor deposition technology [28]. The major part of PNT, composed of cyclic-FF molecules, were closed-top PNT of nanobelt shape having fiber-like structure (Figure 1C and D). Ten to 20% of PNT were open-end hollow PNT [34]. The latter were described by Gazit as composed from linear FF molecules [17].

Wettability studies using envronmental scaning electron microscope (ESEM) allowed us to follow in detail the wetting dynamics of individual PNT. The water condensation process was observed preferentially on the apex of only an open-end PNT (Figure 11A). A high-resolution image (Figure 11B, inset) of a single nanotube clearly revealed the open tip with an outer PNT diameter of 150 nm, possessing a hexagonal structure. This image is an additional evidence for the hexagonal symmetry that was observed for the PNT structure (Figure 7). There was no evidence for nucleation on a majority of nanoarray composed of cyclo-FF fibers. Preferential formation of water droplets at the top of the open-end PNT can be explained by a higher hydrophilicity of the PNT top, compared to its outer wall surface. The model of the open-end PNT exhibits numerous hydrophilic channels of ~10 Å diameter aligned toward the nanotube axis [27]. In addition, the Görbitz's model suggests that the outer wall of the PNT is composed of a mixture of hydrophobic hydrophilic or entirely hydrophobic surface. The nucleation of the water droplets at the apex of the PNT suggests that the outer walls of the linear FF-PNT are predominantly hydrophobic. Direct observation of water droplets on the outer PNT wall is confirmed by our data (Figure 11C).

In order to understand the influence of the hydrophilic channels on the water nucleation, its penetration and macroscopic wettability of the PNT array, we investigated the behavior of cyclo-FF-fibers via ESEM. The cyclic structure leads to a dramatic variation of the wettability properties. No water nucleation sites could be observed on the cyclo-FF-fibers. The first sign of water condensation appeared when the pressure was increased from 5.4 to 6 Torr, creating a large water droplet on top of the surface (Figure 11D) [28]. As described earlier, the nanotubes formed by linear FF are hollow and strongly porous, while the vapor deposition technique gives completely different closed-top peptide fibers formed by cyclic-FF that do not have hydrophilic channels. These results are consistent with the theoretical model [52].

Bioinspired PNT Nanotechnological Applications

Self-assembled peptide nanostructures have been studied by many research groups and were used mainly for biomedical purposes as three-dimensional scaffolds for bone regeneration, dental implants, neural tissue engineering; as biosensors for detection of viruses and other pathogens; as antibacterial agents; and in drug, protein, and gene delivery [8–15].

Another direction of PNT application is on engineering and nanotechnology fields. Gazit proposed an elegant method to use the micro- and nanoporous structure of FF nanotubes for casting coaxial nanowires of silver and gold [16,53].Subsequently, this approach was applied to the synthesis of platinum nanoparticles composites [54], micro-fabricated devices [55], and ink jet technology [56]. One of the most promising applications is the electrochemical technology where two different sorts of PNT devices have been proposed: (i) for biosensing and medical diagnostics [57–59] based on spontaneously grown PNT from solutions [59]. This type of sensors is operated by Faraday electrochemical redox reactions, and (ii) for electrochemical capacitors-SCs [28,34] as promising energy storage devices [60].

One of the critical problems of PNM applications is their thermal and chemical stability. A comprehensive research of PNM stability was conducted by Gazit's and Park's groups [61,62]. Electron microscopy, thermal analysis, circular dichroism, and infrared spectroscopy on two sorts on FF nanotubes and nanowires showed that peptide nanowires are highly stable up to 200 °C and in aqueous solutions (from pH 1 to 14) or in various organic solvents. In contrast, PNT disintegrate at ~100 °C.

Journal of PeptideScience

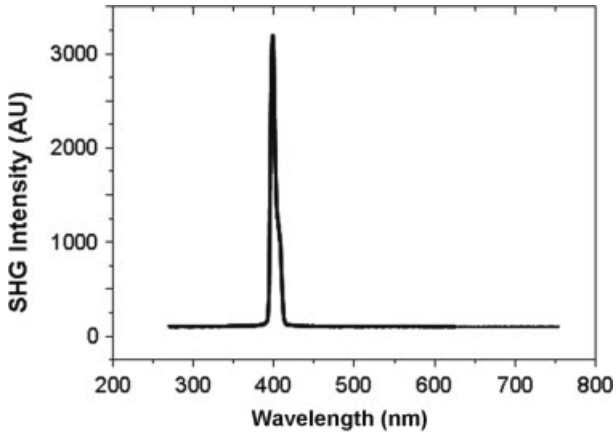

Figure 10. SHG in FF-PNT.

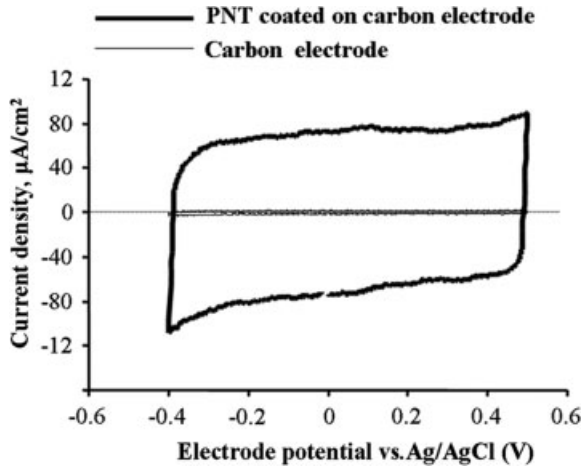

Figure 12. Voltammetry measurements in sulfuric acid electrolyte at a scan rate of 100 mV/s for the carbon electrode (thin gray line) and PNT-modified carbon electrode (black line) showing the capacitance enlargement by 50 times for PNT-coated carbon electrode compared to the uncoated carbon electrode.

Electrochemical PNT-Based Energy Storage Devices – Supercapacitors

SC can operate at high charge/discharge rates over almost an unlimited number of cycles due to negligible Faraday's redox chemical reactions at their electrodes. The SC physical principle is based on creation of electrostatic double layers at the interface electrolyte/electrode providing the distance between these two electrodes defined by Helmholtz layer thickness [63]. Another crucial capacitance's parameter is the SC electrode surface area. Recently, PNT physical vapor deposition technology, compatible with a microelectronic technology, allowed the deposition of unlimited, homogeneous, dense and aligned PNT arrays with high adhesion. This method can be considered as the basis for SC electrode modification. It was found that SC capacitance increased by 12 times for PNT-modified electrodes in comparison to activated carbon and carbon nanotube electrodes with remarkable stability after 10^4 cycles [28]. As we reported recently [34], both the width of the double-layer and the effective surface area of SC electrodes are unambiguously affected by the wettability of the PNT electrode coating. It was found that the PNT fine structure is the critical factor for a strong variation of the SC capacitance. As mentioned in the previous paragraph, the PNT vapor deposited arrays contain two different types of PNT morphologies possessing different wettability. Our experimental data [34] showed that closed-end PNT-peptide fibers do not contribute to SC capacitance and the found capacitance enlargement is due to the open-end hydrophilic hollow PNT.

In Figure 12 voltammetry curves for carbon and PNT-modified carbon electrodes in H_2SO_4 electrolyte are reported. The characteristic anodic and cathodic electrochemical redox Faradaic processes begin at the applied potentials of -0.4 and $+0.5$ V *versus* Ag/AgCl for a vapor deposited PNT electrode. PNT modification of the carbon electrode leads to substantial changes of the SC parameters when the electrical C_{DL} reached $C_{DL} \sim 800\ \mu F/cm^2$, while for the smooth carbon electrode the capacitance was $C_{DL} \sim 16\ \mu F/cm^2$. The C_{DL} discovered in the sulfuric electrolyte exceeds almost twice the SC capacitance in KCl electrolyte [28], where the electrical C_{DL} of PNT reached $C_{DL} = 480\ \mu F/cm^2$. One can assume that the higher current density in H_2SO_4 may be related to the higher mobility of protons.

Pronounced enlargement of the SC capacitance using PNT-modified electrodes combined with the PNT large scale technology promises a fast development in advanced energy storage devices.

Summary

In this review, we present a new approach to fundamental research and nanotechnology applications of bioinspired PNM. This approach is based on the studies of PNM intrinsic physical properties. These physical properties are totally based on the features displayed at the nanoscale level. The crystalline peptide subunits self-assembled into PNM of diverse shapes, are endowed of unique physical properties related to their nanosize dimensions, asymmetric crystalline structure, and porous architecture. Each of

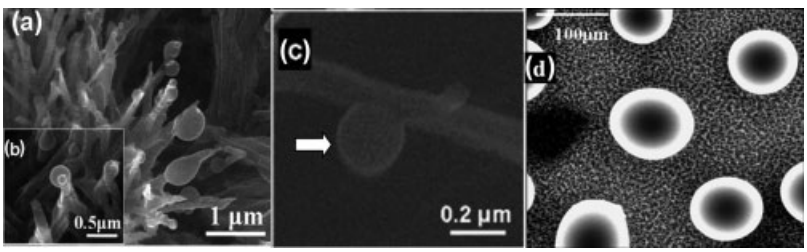

Figure 11. ESEM images of water condensation on the FF-PNT coating. (a) Condensation of water droplets occurs preferentially on the top of the open-end PNT; (b) the insert shows condensation of water on open tip of a PNT tube, showing hexagonal structure of the single FF-PNT; (c) condensation of water on outer surface of FF-PNT; (d) superhydrophobic behavior of closed-end PNT-peptide fibers.

these intrinsic peculiarities of PNM is the basis for the observed physical properties such as quantum confined phenomena, high optical nonlinearity-SHG, strong piezoelectric activity pointing to electrical spontaneous polarization-ferroelectricity, nanoscale wettability, and electrochemical behavior. We firmly believe that the physical effects observed in bioinspired materials may be applied to better understand the basic processes in protein fibers and amyloid fibrils.

These findings permit to propose a new generation of bioinspired nanostructured materials for the applications in the field of nanophotonics, nanopiezoelectricity, and energy storage devices, based on the large scale PNM deposition method.

Acknowledgements

We greatly appreciate biological inspiration by Prof. E. Gazit and for fruitful discussion, as well as assistance of Prof. M. Molotskii. We appreciate contribution of N. Amdursky who performed PNM optical studies.

References

1 Scheibel T. Protein fibers as performance proteins: new technologies and applications. *Curr. Opin. Biotechnol.* 2005; **16**: 427–433.
2 Hearle J. Protein fibers: structural mechanics and future opportunities. *J. Mater. Sci.* 2007; **42**: 8010–8019.
3 Sipe J, Cohen A. Review: history of the amyloid fibril. *J.Struct. Biology.* 2000; **130**: 88–99.
4 Jimenez J, Nettleton E, Bouchard M, Robinson C, Dobson C, Saibil H. The protofilament structure of insulin amyloid fibrils. *PNAS.* 2002; **99**: 9197–9201.
5 Makin O, Serpell L. Examining the structure of the mature amyloid fibril. *Biochem. Soc. Transact.* 2002; **30**: 521–526.
6 Serpell L, Berriman J, Jakes R, Goedert M, Crowther R. Fiber diffraction of synthetic α-synuclein filaments shows amyloid-like cross-β conformation. *Proc. Natl. Acad. Sci. U. S. A.* 2000; **97**: 4897–4902.
7 Perutz M, Finch J, Berriman J, Lesk A. Amyloid fibers are water-filled nanotubes. *Proc. Natl. Acad. Sci. U. S. A.*. 2002; **99**: 5591–5595.
8 Yang Y, Khoe U, Wang X, Horii A, Yokoi H, Zhang S. Designer self-assembling peptide nanomaterials. *Nano Today.* 2009; **4**: 193–210.
9 Gao X, Matsui H. Peptide-based nanotubes and their application in bionanotechnology. *Adv. Mater.* 2005; **17**: 2037–2050.
10 Ulijn R, Smith A. Designing peptide based nanomaterials. *Chem. Soc. Rev.* 2008; **37**: 664–675.
11 Gazit E. Self-assembled peptide nanostructures: the design of molecular building blocks and their technological utilization. *Chem. Soc. Rev.* 2007; **36**: 1263–1269.
12 Zhang S. Fabrication of novel biomaterials through molecular self assembly. *Nat. Biotechnol.* 2003; **21**: 1171–1178.
13 Ghadiri M, Grania J, Milligan R, McRee D, Khazanovitch N. Self-assembling organic nanotubes based on a cyclic peptide architecture. *Nature.* 1993; **366**: 324–327.
14 Hartgerink J, Granja J, Milligan R, Ghadiri MR. Self assembling peptide nanotubes. *J. Am. Chem Soc.* 1996; **118**: 43–50.
15 Bong D, Clark T, Granja J, Ghadiri M. Self-assembling organic nanotubes. *Angew. Chem. Int. Ed.* 2001; **40**: 988–1011.
16 Reches M, Gazit E. Casting metal nanowires within discrete self-assembled peptide nanotubes. *Science* 2003; **300**: 625–627.
17 Reches M, Gazit E. Controlled patterning of aligned self-assembled peptide nanotubes. *Nat. Nanotechnol.* 2006; **1**: 195–200.
18 Reches M, Gazit E. Formation of closed-cage nanostructures by self-assembly of aromatic dipeptides. *Nano Lett.* 2004; **4**: 581–585.
19 Görbitz CH. The structure of nanotubes formed by diphenylalanine, the core recognition motif of A.lzheimer's β-amyloid polypeptide. *Chem. Commun* 2006; 2332–2334.
20 Görbitz C. Structures of dipeptides: the head-to-tail story. *Acta Cryst.* 2010; **B66**: 84–93.
21 Görbitz C. Microporous organic materials from hydrophobic dipeptides. *Chem. Eur. J.* 2007; **13**: 1022–1031.
22 Görbitz C. Peptide structures. *Curr. Opin. Sol. St. Mater. Sci.* 2002; **6**: 109–116.
23 Kitaev Yu, Panfilov A, Smirnov V, Tronc P. Why biomolecules prefer only a few crystal s.tructure. *Phys. Rev. E.* 2003; **67**: 011907.
24 Lang S. Pyroelectric effect in bone and tendon. *Nature.* 1966; **212**: 704–705.
25 Kimura S. Molecular dipole engineering: new aspects of molecular dipoles in molecular architecture and their functions. *Org. Biomol. Chem.* 2008; **6**: 1143–1148.
26 Svelto O. *Principles of Lasers*. Pleneum Press: New York, 1998.
27 Görbitz C. Nanotube formation by hydrophobic dipeptides. *Chem. Eur. J.* 2001; **7**: 5153–5159.
28 Adler-Abramovich L, Aronov D, Beker P, Yevnin M, Buzhansky L, Rosenman G, Gazit E. Self-assembled arrays of peptide nanotubes by vapour deposition. *Nat.Nanotechnol.* 2009; **4**: 849–853.
29 Amdursky N, Molotskii M, Aronov D, Adler-Abramovich L, Gazit E, Rosenman G. Blue luminescence based on quantum confinement at peptide nanotubes. *Nano Lett.* 2009; **9**: 3111–3115.
30 Amdursky N, Molotskii M, Gazit E, Rosenman G. Self-assembled bio-inspired quantum dots: optical properties. *Appl. Phys. Letts.* 2009; **94**: 261907–261910.
31 Amdursky N, Gazit E, Rosenman G. Quantum confinement in self-assembled bio-inspired peptide hydrogels. *Adv. Mater.* 2010; **22**: 2311–2314.
32 Amdursky N, Beker P, Shklovsky J, Gazit E, Rosenman G. Ferroelectric and related phenomena in biological and bioinspired nanostructures. *Ferroelectrics.* 2010; **399**: 107–111.
33 Kholkin A, Amdursky N, Bdikin I, Gazit E, Rosenman G. Strong piezoelectricity in bioinspired peptide nanotubes. *ACS Nano.* 2010; **4**: 610.
34 Beker P, Rosenman G. Bioinspired supercapacitor electrodes with peptide nanotubes. *J Mater Res* 2010; **25**: 20–26.
35 Shklovsky J, Beker P, Amdursky N, Gazit E, Rosenman G. Bioinspired peptide nanotubes: deposition technology and physical properties. *Mater. Sci. Eng. B.* 2010; **169**: 62–66.
36 Gazit E, International Patent Publication Abramovitch L, Aronov D, Rosenman G. Biomolecules vapor deposition provisional patent September 13, 60/960,066, 2007; PCT Patent Application No. PCT/IL2008/001118 filed 13 August 2008.
37 Madou MJ. *Fundamentals of Microfabrication: The Science of Miniaturization*. Taylor & Francis: London, 1997.
38 Wang M, Gates B. Directed assembly of nanowires. *Mater. Today.* 2009; **12**: 3443.
39 Ishihara Y, Kimura S. Nanofiber formation of amphiphilic cyclic tri-β-peptide. *J. Pept. Sci.* 2010; **16**: 110–114.
40 Nye J. Oxford Science Publications *Physical Properties of Crystals: Their Representation by Tensors and Matrices*. Oxford Science Publications: 2004.
41 Lemanov V, Popov S, Pankova G. Piezoelectric properties of crystals of some protein aminoacids and their related compounds. *Solid State. Phys.* 2002; **44**: 1929–1935.
42 Fukada E, Yasuda I. On the piezoelectric effect of bone. *J. Phys. Soc. Jpn.* 1957; **12**: 1158–1162.
43 Fukada E. Piezoelectric properties of biological materials. *Q. Rev. Biophys.* 1983; **16**: 59–87.
44 Lang S, Marino A, Berkovic G, Fowler M, Abreo K. Piezoelectricity in the human pineal gland. *Bioelectroch. Bioener.* 1996; **41**: 191–195.
45 Halperin C, Mutchnik S, Agronin A, Molotskii M, Urenski P, Salai M, Rosenman G. Piezoelectric properties of bones studied in nanometer scale. *Nano Lett.* 2004; **4**: 1253–1256.
46 Harnagea C, Vallieres M, Pfeffer C, Wu D, Olsen B, Pignolet A, Legare F, Gruverman A. Two-dimensional nanoscale structural and functional imaging in individual collagen type I fibrils. *Biophys. J.* 2010; **98**: 3070–3077.
47 Nikiforov M, Thompson G, Reukov V, Jesse S, Guo S, Rodriguez B, Seal K, Vertegel A, Kalinin S. Double-layer mediated electromechanical response of amyloid fibrils in liquid environment. *ACS Nano.* 2010; **4**: 689–698.
48 Jolandan M, Yu Min-Feng. Nanoscale characterization of isolated individual type I collagen fibrils: polarization and piezoelectricity. *Nanotechnol.* 2009; **20**: 85706–85712.
49 Williams R, Zipfel W, Webb W. Interpreting second-harmonic generation images of collagen I fibrils. *Biophys. J.* 2005; **88**: 1377–1386.
50 Pfeffer C, Olsen B, Le'gare F. Multimodal nonlinear optical imaging of collagen arrays. *J. Struct. Biol.* 2008; **164**: 140–145.

51 Lee J, Ryu J, Park C. Bio-inspired fabrication of superhydrophobic surfaces through peptide self-assembly. *Soft Matter.* 2009; **5**: 2717–2720.
52 Joshi KB, Verma S. Participation of aromatic side chains in diketopiperazine ensembles. *Tetrahedron Lett.* 2008; **49**: 4231–4234.
53 Carny O, Shalev D, Gazit E. Fabrication of coaxial metal nanocables using a self-assembled peptide nanotube scaffold. *Nano Lett.* 2006; **6**: 1594–1597.
54 Song Y, Challa SR, Medforth CJ, Qiu Y, Watt RK, Pena D, Miller JE, van Swol F, Shelnutt JA. Synthesis of peptide-nanotube platinum-nanoparticle composites. *Chem. Commun.* 2004; 1044–1045.
55 Sopher N, Abrams Z, Reches M, Gazit E, Hanein Y. Integrating peptide nanotubes in micro-fabrication processes. *J. Micromech. Microeng.* 2007; **17**: 2360–2365.
56 Adler-Abramovich L, Gazit E. Controlled patterning of peptide nanotubes and nanospheres using inkjet printing technology. *J. Pept. Sci.* 2008; **14**: 217–223.
57 Yemini M, Reches M, Gazit E, Rishpon J. Peptide nanotube-modified electrodes for enzyme-biosensor applications. *Anal. Chem.* 2005; **77**: 5155–5159.
58 Yemini M, Reches M, Rishpon J, Gazit E. Novel electrochemical biosensing platform using self-assembled peptide nanotubes. *Nano Lett.* 2005; **5**: 183–186.
59 Adler-Abramovich L, Badihi-Mossberg M, Gazit E, Rishpon J. Characterization of peptide nanostructure-modified electrodes and their application for ultrasensitive environmental monitoring. *Small.* 2010; **6**: 825–831.
60 Burke A. Ultracapacitors: why, how, and where is the technology. *J. Power Sources* 2000; **91**: 37–50.
61 Adler-Abramovich L, Reches M, Sedman V, Allen S, Tendler S, Gazit E. Thermal and chemical stability of diphenylalanine peptide nanotubes: implications for nanotechnological applications. *Langmuir.* 2006; **22**: 1313–1320.
62 Ryu J, Park CB. High stability of self-assembled peptide nanowires against thermal, chemical, and proteolytic attacks. *Biotechnol. Bioeng.* 2010; **105**: 221–230.
63 Conway B. *Electrochemical Supercapacitors: Scientific Fundamentals and Technological Applications*. Kluwer Academic/Plenum Publishers: New York, 1999.

